NASA-CR-203114

SwRI Proposal No. 15-5614
December 31, 1996

An Annual Report for

NASA Planetary Astronomy Lunar Atmospheric Imaging Study
NAGW-3481

Submitted to:

Planetary Astronomy Program
NASA Solar System Exploration Division
NASA Headquarters
Code SL
Washington, DC 20546

Prepared by:

S. Alan Stern
Southwest Research Institute
Division 15 Boulder Extension Office
Geophysical, Astrophysical, and Planetary Sciences Section
1050 Walnut, Suite 426
Boulder, Colorado 80302
303/546-9670 FAX 303/546-9687

SOUTHWEST RESEARCH INSTITUTE
Instrumentation and Space Research Division
6220 Culebra Road, San Antonio, Texas 78238
(210) 684-5111 • FAX (210)647-4325

Project Background and Results

With \$38 40K yr^{-1} of support during the past three-year Planetary Astronomy cycle, we have conducted a program of research focused on studies of the lunar atmosphere. Here we summarize the background and results obtained from the lunar atmosphere work we have undertaken.

A1.1 Lunar Atmosphere Research Background

The lunar atmosphere is a nearby, observationally accessible analog to the two other tenuous, surface boundary exospheres in the solar system: those at Mercury and Io. Studies of the lunar atmosphere reveal details about the workings of tenuous exospheres across the solar system, and establish a more well-rounded understanding of the Moon.

Although the lunar atmosphere is known to consist of neutral Ar, He, Na, and K, only Na and K display bright resonance fluorescence emissions observable from groundbased telescopes. The Na and K D-line emissions have been studied spectroscopically since their discovery in 1987 (Potter & Morgan 1988a; Tyler, Kozlowski, & Hunten 1988), and display characteristic strengths of 4 and 2 kilo-Rayleighs (kR), respectively, which correspond to typical Na and K column abundances of $8\pm3\times10^8$ cm^{-2} and $1.4\pm0.3\times10^8$ cm^{-2}, respectively. There is wide agreement that the dominant sink for Na and K is photoionization (cf., Morgan & Stern 1991). However, a complex and only partially complete picture has developed with regard to the source processes acting in this fascinating surface boundary exosphere: Apparently, both thermal and nonthermal source processes are at work (e.g., Potter & Morgan 1988b; Sprague et al. 1992; Stern & Flynn 1995). For a more detailed discussion, see the excellent summary and description of state of the art models of the lunar atmosphere published by Smyth & Marconi (1995).

The research we have undertaken in the Planetary Astronomy program has concentrated on studies of the energetics and composition of the lunar atmosphere. This has been accomplished by imaging sodium near the lunar surface and by engaging in spectroscopic searches for new species in the lunar atmosphere. The main objectives of our imaging work have been to develop this new tool and to exploit it to better characterize the composition, vertical and horizontal structure, and temporal variations of the lunar sodium. The imaging program is, to our knowledge, unique, in that it obtains information on the 3-dimensional spatial distribution of Na near the surface. The new species search, which we conducted using a Coudé spectrograph, has twin objectives. The first goal is simply to obtain a better census of the lunar atmosphere; the second goal is to use the information gained to better constrain the source processes generating the lunar atmosphere.

A1.2 Results of Our Lunar Atmospheric Imaging Work

The first imaging observations of the lunar Na exosphere were reported by Mike Mendillo's group (Mendillo et al. 1991; Flynn & Mendillo 1993). The coronographic, wide-field Na imaging technique that Mendillo and co-workers developed has produced a steady stream of valuable results, including dramatic images of Na at altitudes as great as $9R_M$ (Mendillo & Baumgardner 1995). Although useful for studying the high-altitude lunar atmosphere, such observations are limited in some important respects by their use of an occulting mask that blocks both the Moon and lunar atmosphere below ~800 km altitude.

In our previous three-year proposal, we proposed to develop a complementary technique

capable of imaging the low-altitude Na and K in the lunar atmosphere. This technique does not use a coronograph to block the surface and near-surface atmosphere. Since 1993, this technique has been refined into a tool for the exploration of the Na distribution, and we are ready to extend it to K.

To obtain high-resolution images of Na I D emission in the lunar atmosphere, we employ a CCD camera on meter-class telescopes. To make the necessary contrast improvement between the atmospheric Na I D_2 signal (5890 Å), and the much brighter lunar surface albedo, we take three steps. First, we use a Na interference filter to reject surface-scattered sunlight outside all but a narrow (3 Å) range around the Na D_2 line. Our image-quality filter was optimized for the $f/13$ beam of the McDonald 0.9 m and a nominal observing temperature of 13°C. The filter is tilt-controlled to ensure proper registration on the Na I emission line as ambient temperature conditions in the camera change. Second, as shown in Figure 1, we point the CCD field of view (FOV) just to the dark side of the lunar terminator. This eliminates essentially all of the strong (~10 MR/Å) background normally present from the daylit lunar surface, so that only backscattered earthshine remains. Whereas this technique largely eliminates the surface backscatter, atoms on ballistic trajectories above the dark side of the terminator remain illuminated by sunlight and can therefore still fluoresce; as a result, virtually all of the (kR-strength) atmospheric Na emission remains available for detection. As a result, the atmosphere/surface contrast ratio is improved dramatically. The third aspect of our observing technique is designed to minimize the contribution of earthshine illumination: we observe when the Moon is within 5 days of full; as a result the Earth as seen from the Moon is almost new.

Since late 1993 when funding for this program was initiated, we have made four Na imaging observing runs. The resulting dataset consists of over 200 Na images made in pole-to-pole strips along the terminator. Initial results from these runs were reported in two talks (Stern & Flynn 1994; Flynn & Stern 1994a) at the 1994 DPS meeting. In a subsequent *The Astronomical Journal* paper (Stern & Flynn 1995), we described this high-resolution, low-altitude imaging technique in some detail, and presented a first set of results.

In the *AJ* paper we reported that when we constructed a simple, Chamberlain exosphere model, no isothermal Na population could fit the Na brightness profiles. Instead, as shown in Figure 2, both cold (i.e., barometric) and hot (i.e., suprathermal) populations were needed to fit the radial intensity profiles. This proves that multiple source processes are at work in the lunar atmosphere. As we describe below, these data also demonstrate that the mixing ratio of the two thermal components varies with latitude, which in turn provides new clues to the identity of the specific source processes at work.

The possible existence of both (thermal and suprathermal) Na populations had been debated previously (e.g., Morgan & Shemansky 1991; Kozlowski et al. 1990; Sprague et al. 1992), but no observations had unambiguously detected and resolved both the thermal and nonthermal populations simultaneously. The key to detecting both thermal components was our ability to sample the atmosphere virtually down to the surface.

As noted above, in addition to the simple existence of two thermal components, we also found that the mixing ratios and temperatures of the two components vary systematically with latitude. Although the latitudinally dependent mixing ratio systematics provide a new clue to the identity of the different source mechanisms at work, we cannot say we understand the cause of the latitudinal systematics at this time.

We also discovered that our data also contains evidence indicating for the first time (i) that the Moon generates Na column gradients above Mare and highland units, and (ii) temporal fluctuations in the Na column abundances on 1000-second timescales above the

terminator, suggesting coherent dynamics in the low-altitude Na.[1]

In summary, we have collected a database of Na images that fills a unique niche for studying the lunar atmosphere. Publihsed results from this database have yielded definitive evidence for a two-component Na thermal distribution which displays previously-unknown latitudinal systematics. The database also contains evidence for gradients in the Na column that are apparently correlated with underlying surface unit properties, and also for interesting dynamics near the terminator.

A1.3 Results of Our Lunar Atmospheric Species Search

Beginning in 1994, we have also undertaken a spectroscopic survey to determine what other metal species may be present in the lunar atmosphere. By metals, we mean any element bound in rocks and minerals on the lunar surface except H and He. Our survey was motivated by the desire to rectify the present-day inconsistency between total atmospheric abundance measurements made by Apollo *in situ* instruments, and the much lower total atmospheric abundance of the compositionally identified species. Whereas the Apollo surface cold cathode gauge experiments determined that the nighttime surface number density can exceed 2×10^5 cm^{-3}, the four species detected to date (He, Ar, Na, and K) together compose less than 20% of the total density. Despite this mismatch between total number density and the combined number density of the four total detected species, it is often not recognized that most of the lunar atmosphere remains compositionally unidentified.

Because atmospheric Na and K are primarily generated by exogenic source processes acting on the surface layer, it is natural to suspect that other species in the surface may also be injected into the lunar atmosphere by the same source processes.[2] Apollo lunar sample returns have shown that many elements are comparable in abundance to, or more abundant than, Na and K in lunar soils (cf., Taylor 1982). For a surface that has reached an equilibrium composition under long-term bombardment by solar wind particles, one might expect surface sputtering to reflect the bulk composition of the surface (Johnson & Baragiola 1991). Such an equilibrium would imply that atmospheric abundance ratios from mature surface units will be stoichiometric for those species produced by atomic sputtering.

As a planning tool for our observations we constructed a model of possible lunar atmosphere abundances. Given the absence of laboratory data to support the construction of a unique non-stoichiometric model, we constructed a stoichiometric model (cf., Flynn & Stern 1996). We consider this a crude but valid first approach to predicting the abundances of other atomic neutrals derived from the surface. Table 1 shows the established Na parameters and our predictions for a suite of eight potentially detectable species based on this simple model. Notice in Table 1 that the column abundances and brightnesses predicted by this model for K agree with existing K observations (cf., Potter & Morgan 1988a); the Na/K ratio is stoichiometric. Notice also that the predicted brightnesses for Si, Ca, Fe, and Ti are comparable to or brighter than the observed Na, indicating the feasibility of a search. The predicted values for emission lines of several other potential species, including Al, Ba, and the other alkalis, Li, Rb, and Cs were also found to be favorable for a search.

In 1994 and 1995 we proposed and were granted time at McDonald to search for emissions from this suite of species (and of course to search the bandpasses we observed for

[1] These dynamics are qualitatively reminiscent of the Ar winds detected by the Apollo 17 ALSEP mass spectrometer (Hodges et al. 1973).

[2] cf., also Feldman & Morrison (1991) for a discussion of Apollo 17 UVS-derived upper limits on C, H, O, N, S, Kr, Xe, and CO.

other possible emissions). The July 1994 observations targeted only Na, Ca, Ti, and Li, and were taken with the McDonald Observatory 2.7 m Coudè spectrograph at R≃60,000, using an 800×800 pixel CCD. The spectrograph slit had a projected length of ≃20″. Order-separating filters were used. Each resulting spectrum encompassed ≃ 10 Å centered on the strongest predicted resonant scattering emission line of these four species. The March 1995 observations were obtained by using the McDonald 2.1 m Cassegrain echelle spectrograph. This instrument cross-disperses many separate orders on an 800x1200 CCD, giving simultaneous access to a broad bandpass. We obtained data at three grating positions covering 3705–3985 Å, 5510–6913 Å, and 6900–9675 Å.

The results of these two observing runs were reported at talks given at the 1994 Fall AGU and 1995 LPSC meetings, and in a refereed paper that is now in press at *Icarus* (Flynn & Stern 1996). Figure 3 shows some sample spectra from our 1996 paper. Our search was more sensitive than required to detect the model predictions for most of the species listed in Table 1. Despite this, no new atmospheric species were detected. The measured upper limits on emission brightnesses for 7 of these 9 species fall significantly below the values predicted from a simple stoichiometric model (cf., Table 1). Figure 4 shows the degree to which the species depart from stoichiometry; Figure 4 also gives the ratio of the observed upper limits on atmospheric abundances, relative to their stoichiometrically predicted values.[3] These results show that many other atomic neutrals, including the other alkalis, Li, Cs, and Rb are strongly substoichiometric, in contrast to K.

The fact that Na and K are abundant, and stoichiometric relative to one another, whereas other species (Si, Al, Ca, Fe, Ti, and Li – which is also volatile, like Na and K) are neither, clearly provides an important set of clues to the surface processes that produce the lunar atmosphere. It may indicate that the surface layer may not have reached radiation-exposure equilibrium. Alternatively, the lack of other abundant surface atoms in the atmosphere may support the suggestion that chemical sputtering, which favors high vapor pressure species like Na and K, is a key source process (cf., Potter 1995), or it may be that the metal species we searched for may be preferentially injected into the atmosphere as molecular oxide fragments (e.g., CaO, TiO, TiO_2, etc.) rather than atoms, in which case we would not have detected them. These results provide important new food for thought, and beg deeper analysis. However, we think it is likely that until additional species *are* discovered in the lunar atmosphere, it will likely not be possible to uniquely constrain the source processes at work and therefore finally resolve why Na and K predominate over everything so far identified except noble gases.

A1.4 Related Activities

In addition to the six observing runs, four technical talks, and two refereed papers that we have completed, several other accomplishments related to this Planetary Astronomy program deserve mention: (i) PI Stern authored a 2500+ word, popular article on the lunar atmosphere for *Astronomy* magazine (Stern 1994). (ii) PI Stern and CoI Flynn organized the first-ever International Lunar Atmosphere Week (ILAW); ILAW I took place 13–19 September 1995, and succeeded in obtaining coordinated imaging and spectroscopy of the lunar atmosphere by four separate groups, including our own. (iii) PI Stern participated in a search for new metal species in Io's atmosphere; this search yielded stringent new limits on a dozen possible species and a paper has been submitted to *Icarus* for publication (Na,

[3] We note that a similar search at Mercury would be particularly useful. Sprague has set upper limits on Ca and Li, but the other species remain wholly unconstrained at Mercury.

Trafton, Barker, & Stern 1996). As in the lunar atmosphere, Na and K are preferentially produced at Io. And (iv) we were honored to be invited by *Reviews of Geophysics* to submit a review article on the lunar atmosphere for publication in 1997.

Table 1. Stoichiometric Model Predictions

Species	λ_0^a (Å)	Surf Abundance[b] Ratio	g-factor[c] (sec^{-1})	Col Abundance[d] Est. (cm^{-2})	Brightness[e] Est. (kR)
Na I[f]	5889	1	0.54	4.8×10^9	2.6
K I[f]	7699	0.3	1.7	6.3×10^8	1.0
Si I	3905	50	0.058	2.5×10^{11}	15.
Al I	3961	30	0.037	5.7×10^9	0.21
Ca I	4226	16	0.49	2.5×10^{10}	12.
Fe I	3719	8	0.0061	6.3×10^{11}	3.8
	3859	8	0.012	6.3×10^{11}	7.6
Ti I	5036	1	0.68	2.5×10^9	1.7
Ba I	5536	0.03	11.	1.2×10^4	0.00013
Li I	6708	0.005	16.	2.9×10^6	0.046
Rb I[g]	7800	0.0009	-	-	-
Cs I[f]	8521	0.00004	-	-	-

Adapted from Flynn & Stern (1996). Notes: (a) Wavelength. (b) Surface abundance relative to Na (Taylor 1982). (c) Scattering efficiency. (d) Estimated atmospheric line-of-sight column abundance at 40 km (20″) above the subsolar limb at quarter Moon based on relative surface abundance, ionization lifetime, and altitude distribution from a Chamberlain exosphere at 1000 K. (e) Estimated emission brightness at 40 km. (f) Na and K have been observed via groundbased spectroscopy and direct imaging. (g) No predictions were made for Rb I and Cs I because the atomic data could not be located.

References

Allen, C.W., *Astrophysical Quantities*, Athlone, London, 1973.

Chamberlain, J.W., and D.M. Hunten, in *Theory of Planetary Atmospheres*, pp. 330-415, Academic Press, Boston, MA, 1987.

Feldman, P.D., and D. Morrison, *GRL*, 18, 2105, 1991.

Flynn, B.C., and M. Mendillo, *Science*, 261, 184, 1993.

Flynn, B.C., and S.A. Stern, *BAAS*, 25, 1994a.

Flynn, B.C., and S.A. Stern, Lunar and Planetary Science Conference XXV, pp 377, 1994b.

Flynn, B.C., and S.A. Stern, *Icarus*, in press, 1996.

Hapke, B., *AJ*, 71, 333-339, 1966.

Hunten, D.M., T.H. Morgan, and D. Shemansky, in *Mercury* (F. Vilas and C.R. Chapman, eds), pp. 562, University of Arizona Press, Tucson, Ariz., 1988.

Johnson, R.E., and R. Baragiola, *GRL*, 18, 2169, 1991.

Killen, R.M., and T.H. Morgan, *Panel. Space Sci.*, submitted, 1996.

Kozlowski, R.W.H., A.L. Tyler, and D.M. Hunten, *GRL*, 19, 642, 1990.

Mendillo, M., J. Baumgardner, and B. Flynn, *GRL*, 18, 2097, 1991.

Mendillo, M., and J. Baumgardner, *Nature*, 377, 404, 1995.

Morgan, T.H., and D.E. Shemansky, *JGR*, 96, 1351, 1991.

Morgan, T., and S.A. Stern, *EOS*, 72, 522, 1991.

Na, C.Y., L.M. Trafton, E.S. Barker, and S.A. Stern, *Icarus*, submitted, 1996.

Potter, A.E., *GRL*, 22, 3289, 1995.

Potter, A.E., and T.H. Morgan, *Science*, 241, 675, 1988a.

Potter, A.E., and T.H. Morgan, *GRL*, 15, 1515, 1988b.

Smyth, W.H., and M.L. Marconi, *ApJ*, 443, 371, 1995.

Sprague, A., R. Kozlowski, D. Hunten, W. Wells, and F. Grosse, *Icarus*, 96, 27, 1992.

Stern, S.A., *Astronomy*, November, 1993, 36.

Stern, S.A., and B.C. Flynn. *BAAS*, 25, 1994.

Stern, S.A., and B.C. Flynn, *AJ*, 209, 835, 1995.

Taylor, S.R., *Planetary Science: A Lunar Perspective*, Lunar & Planetary Institute, Houston, 1982.

Tyler, A.L., R.W. Kozlowski, and D.M. Hunten, *GRL*, 15, 1141, 1988.

Figure Captions

Figure 1: Schematic illustrating the observing geometry. There is not enough contrast to detect the atmosphere against the bright lunar surface, so observations are made just to the dark side of the lunar terminator. These images were taken between quarter phase and full Moon, when backscatter from the Earth-illuminated portion of the lunar surface is at a minimum.

Figure 2: Radial intensity cuts from each of the images analyzed. Each image was corrected for vignetting, bias, gain, and scattered light. Plotted with each cut is the best two-temperature fit. In panel (a), 3σ lower limits for each temperature are given, where σ is the random error in the data. In panels (b) (d), the 3σ uncertainties in each temperature are given in parentheses. Each temperature component is shown individually along with the combined fit. The percentages for each temperature refer to the fractional abundances at the surface.

Figure 3: Top: Spectra taken in July 1994 near the resonant lines of Na (*left*) and Li (*right.*) *Top*: Spectra taken of the lunar surface 20″ from the subsolar limb. *Middle*: Spectra taken 20″ (40 km) above the subsolar limb, showing terrestrial atmospheric scattering of the lunar surface continuum, and in the case of Na lunar atmospheric emission features. *Bottom*: Difference of top and middle panels showing strong Na emission features at 5890 Å and 5896 Å, and a non-detection of Li. The signal-to-noise ratio for the D_2 line (5890 Å) is approximately 100. The 5σ upper limit for Li is indicated. (Figure from Stern & Flynn 1995.)

Figure 4: Top: Line-of-sight column abundances at 40 km above the limb for Si, Al, Ca, Fe, Ti, and Li relative to Na from both the stoichiometric model (filled circles) and the observations (triangles). The detected value for K is within a factor of 2 of the predicted stoichiometric value. *Bottom*: Ratios of observed upper-limit column abundances to predicted values. A ratio of unity indicates stoichiometric behavior relative to Na. Arrows denote that values are upper limits in the cases of Si, Al, Ca, Fe, Ti, and Li. Note that the K value is within a factor of 2 of unity. (Figure from Flynn & Stern 1996.)

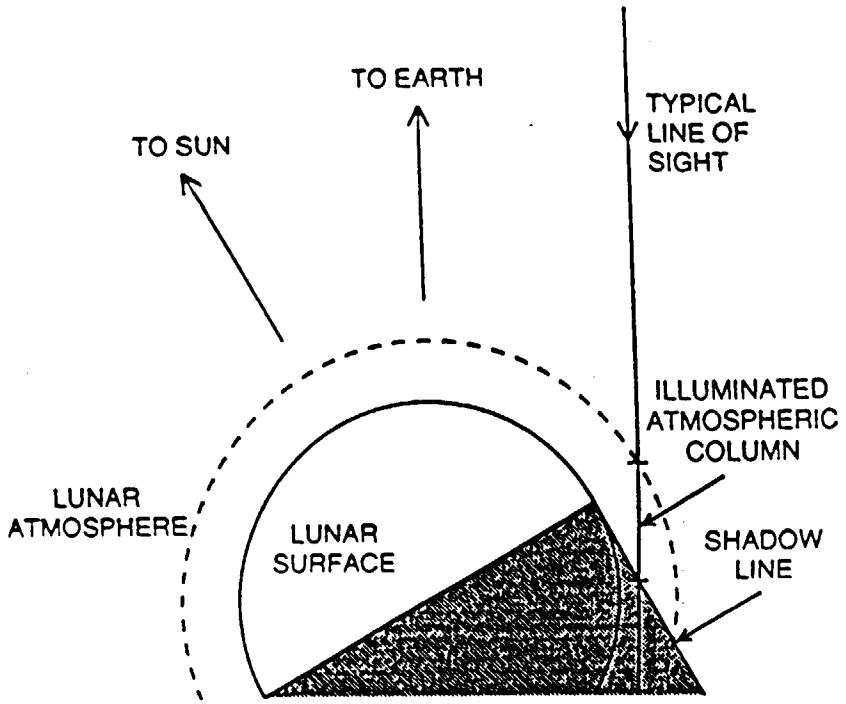

NOT TO SCALE

Schematic illustrating the observing geometry. There is not enough contrast to detect the atmosphere against the bright lunar surface, so observations are made just to the dark side of the lunar terminator. The images are taken between quarter phase and full Moon, when backscatter from the Earth-illuminated portion of the lunar surface is at a minimum. During our observations, the Sun–Moon–Earth phase angle was 33°.

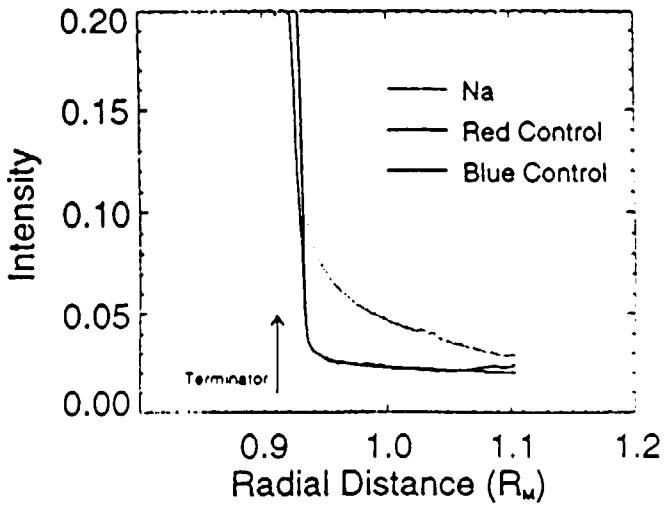

Radial cuts of images taken through each of the three filters. The three images were taken with the same pointing separated by ~1 min time intervals. Each image was corrected for vignetting, bias, and pixel-to-pixel gain differences in the standard way. The control images were scaled to correct for differences in filter area and in the solar spectrum over the filter bandpasses. The clearly increasing ramp of intensity toward the terminator in the Na image is the signature of Na detection. Intensities were not calibrated and are shown in arbitrary units.

FIGURE 1

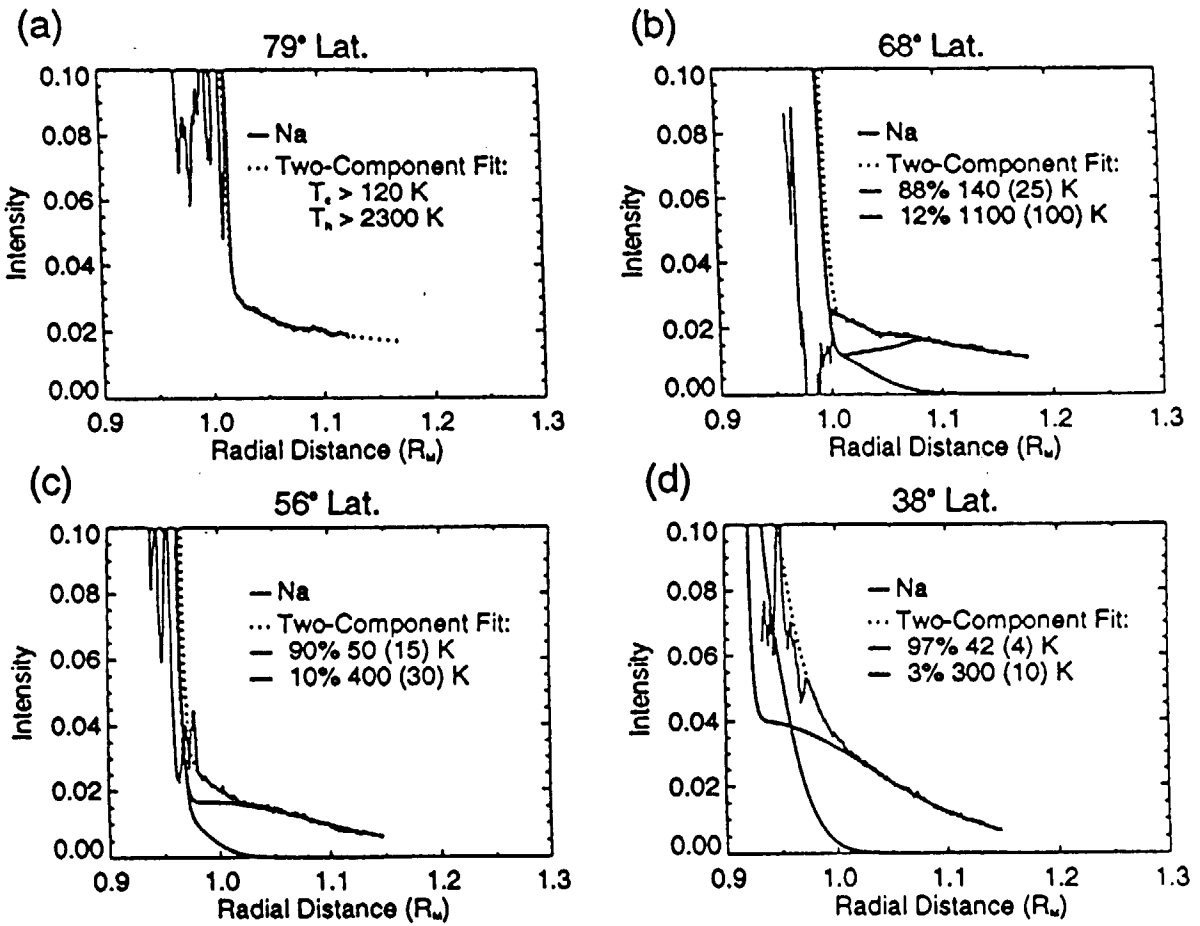

Radial intensity cuts from each of the four images analyzed. Each image was corrected for vignetting, bias, gain, and scattered light. As in Fig. 2, the intensities are shown in arbitrary units. Plotted with each cut is the best two-temperature fit. In panel (a), 3σ lower limits for each temperature are given, where σ is the random error in the data. In panels (b)–(d), the 3 σ uncertainties in each temperature are given in parentheses. Each temperature component is shown individually along with the combined fit. The percentages for each temperature refer to the fractional abundances at the surface.

FIGURE 2

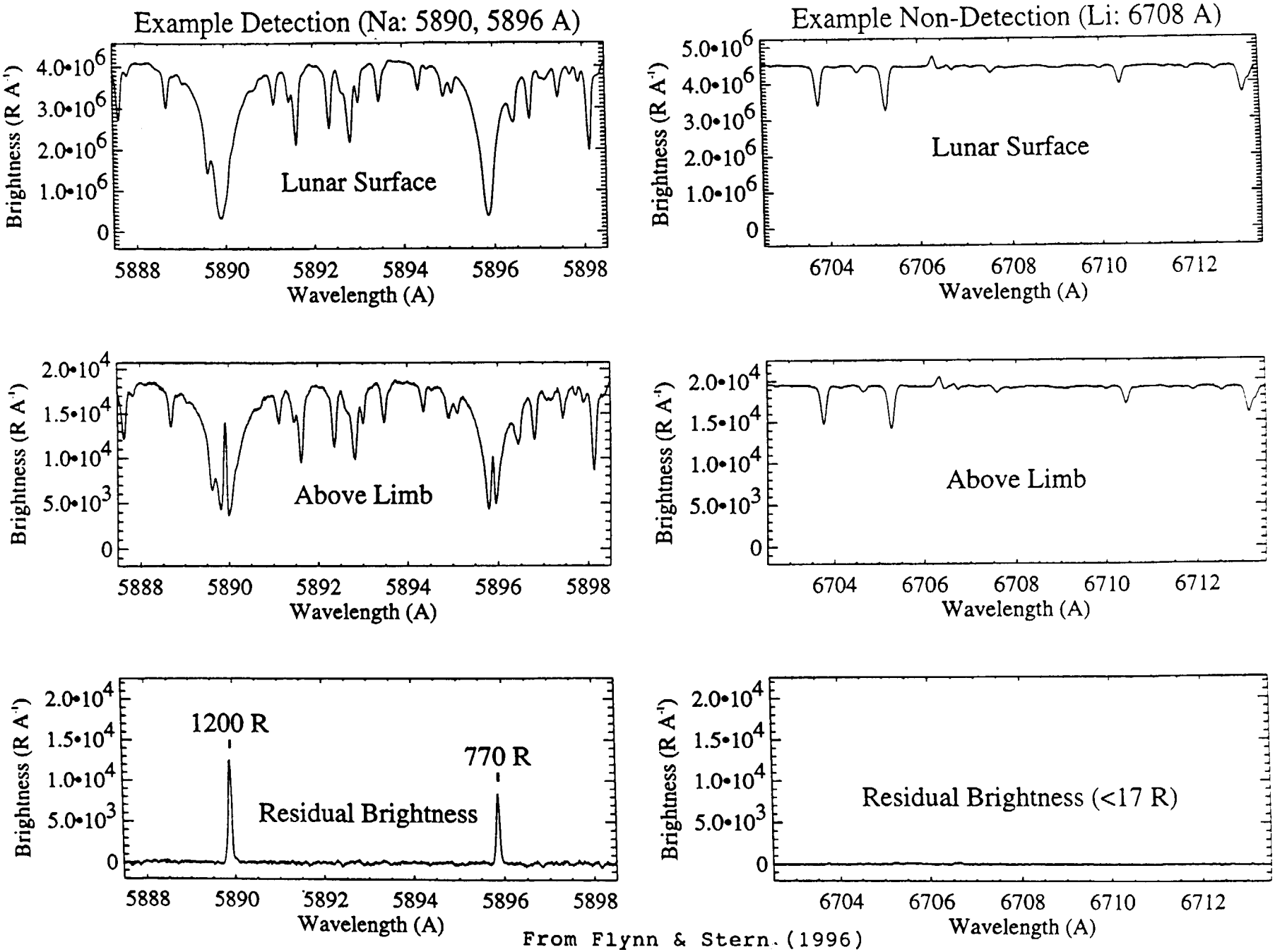

From Flynn & Stern (1996)

FIGURE 3

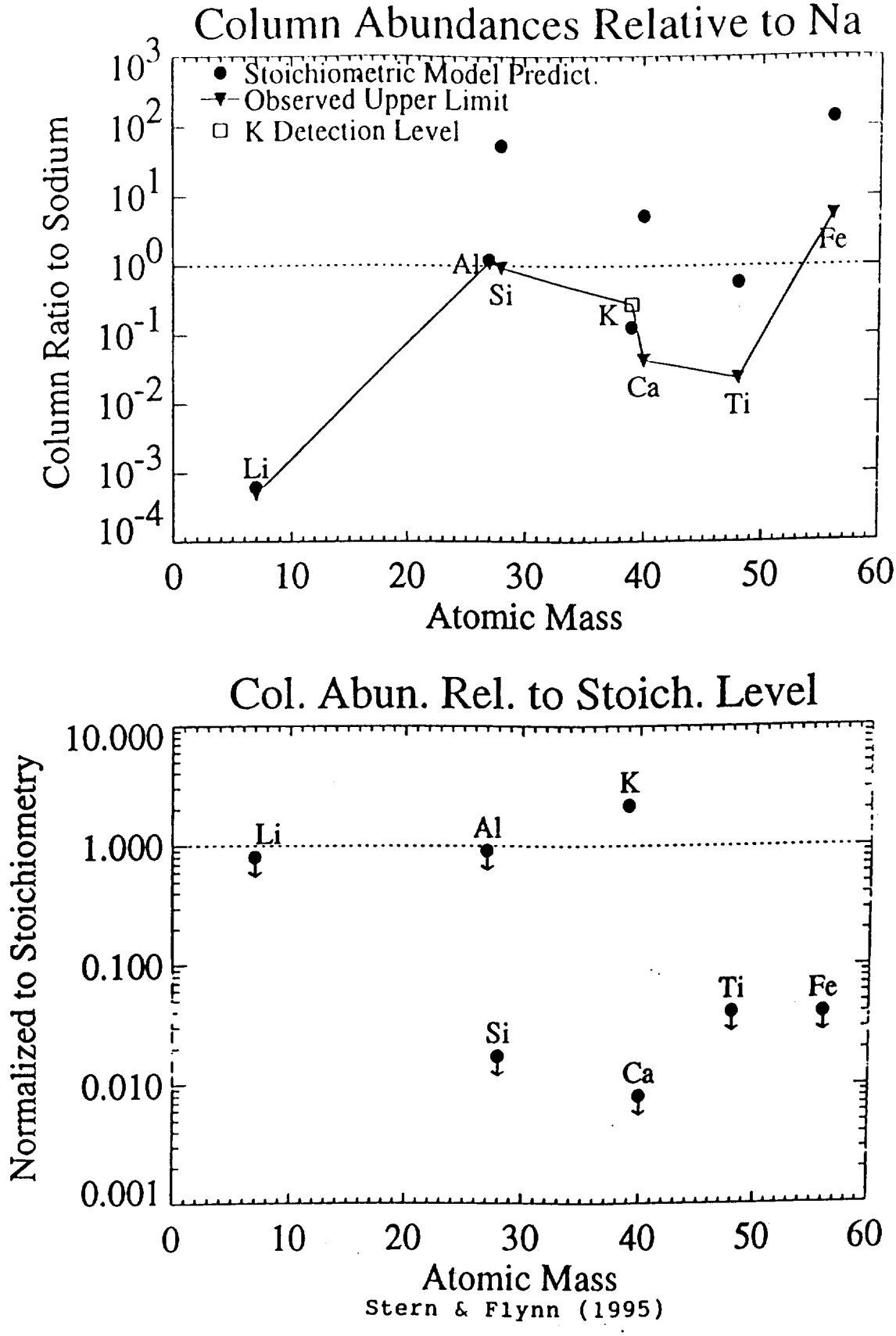
Column Abundances Relative to Na
Stoichiometric Model Predict.
Observed Upper Limit
K Detection Level
Column Ratio to Sodium
10^3
10^2
10^1
10^0
10^{-1}
10^{-2}
10^{-3}
10^{-4}
Li
Al
Si
K
Ca
Ti
Fe
0
10
20
30
40
50
60
Atomic Mass
Col. Abun. Rel. to Stoich. Level
Normalized to Stoichiometry
10.000
1.000
0.100
0.010
0.001
Li
Al
K
Si
Ca
Ti
Fe
0
10
20
30
40
50
60
Atomic Mass
Stern & Flynn (1995)

FIGURE 4

PAPER 1

An Initial Spectroscopic Survey of Metallic Species Abundances in the Lunar Atmosphere

B. C. Flynn[1] and S. A. Stern[1]
Southwest Research Institute, Boulder, Colorado

Received _____; accepted _____

Submitted to *Geophysical Research Letters*, 1995.

Short title: LUNAR ATMOSPHERE ABUNDANCES

[1]Guest Observers, University of Texas McDonald Observatory

Abstract. We present preliminary results of an ongoing effort to determine the degree that metal abundances in the lunar atmosphere are stoichiometric, that is, reflective of the lunar surface composition. From Apollo sample returns, we know that several species are more abundant in the lunar surface than either Na or K [*Taylor*, 1982], which are the only atmospheric constituents to have been observed from Earth. By simple stoichiometric arguments, one predicts the relatively abundant lunar *surface* constituents such as Si, Al, Ca, Mg, Fe, and Ti to be more abundant in the lunar atmosphere than both Na and K. Using the coudé spectrograph of the 2.7 m reflector at the University of Texas McDonald Observatory, we investigated this hypothesis by searching for solar resonant scattering lines of Ca (4227 Å), Ti (5036 Å), and Li (6708 Å). Spectra were taken 20 arcsec above the subsolar limb of the Moon near last quarter on 30 July 1994. Upper limits were obtained for Ca (<360 Rayleighs), Ti (<120 Rayleighs), and Li (<30 Rayleighs). In the cases of Ca and Ti, these upper limits are more than an order of magnitude lower than the simple stoichiometric model predicts. For Li, the upper limit is about a factor of two below the stoichiometric model prediction. We conclude that the lunar atmosphere is not entirely stoichiometric, and we interpret these results as indicating that the mechanism(s) that produce the lunar Na and K atmosphere may somehow favor those species over some more or comparably abundant lunar surface species, and atmospheric searches for other abundant lunar surface species such as Si, Al, and Mg should prove enlightening.

Introduction

The lunar atmosphere was first detected by Apollo instruments. The Apollo 17 surface mass spectrometer identified both Ar and He, with Ar densities reaching at least 4×10^4 cm^{-3}. The Apollo 17 UV Spectrometer obtained upper limits on the atmospheric abundances of several other species, such as H, C, N, and O [*Feldman and Morrison*, 1991], but all were below the 2×10^4 cm^{-3} level. However, total pressure measurements indicated densities exceeding 10^6 cm^{-3}, suggesting that the lunar atmosphere remains largely compositionally unidentified [cf., *Morgan and Stern*, 1991].

More recently, Potter and Morgan discovered resonant scattering emissions from neutral Na and K through groundbased spectroscopy, making it possible to study the lunar atmosphere from the Earth [*Potter and Morgan*, 1988a]. Subsequent observations and modeling studies of the distribution of Na around the Moon have shown that the Na is largely suprathermal in nature [e.g., *Potter and Morgan*, 1988b; *Sprague et al.*, 1992; *Flynn and Mendillo*, 1995], although there is also an underlying thermal component close to the surface [*Stern and Flynn*, 1995]. The suprathermal nature of the Na seen in most observations indicates that an energetic production process, such as solar wind sputtering, photodesorption, or micrometeorite impact vaporization, is responsible for releasing Na from the lunar surface [*Morgan and Shemansky*, 1991; *Sprague et al.*, 1992]. Observations of Na made before, during, and after lunar passage through the Earth's magnetotail have been used to show that solar wind sputtering may be the major source of Na in the lunar atmosphere [*Potter and Morgan*, 1994].

This paper concerns the first results from a spectroscopic search for new species in the lunar atmosphere that we are conducting. This survey is motivated by our desire to better understand both the source mechanisms that generate the lunar Na/K exosphere, and to rectify the present-day inconsistency between total abundance measurements made by Apollo *in situ* instruments, and the much lower abundance of the compositionally identified species. In particular, Apollo surface cold cathode gauge

experiments determined that the daytime surface number density can exceed 10^6 cm^{-3}. However, the four species detected to date (He, Ar, Na, and K) together total to <10% of this value. Interestingly, the Na and K, which are the best known lunar atmosphere species, together total <100 cm^{-3}. It is often not recognized that over 90% of the lunar atmosphere remains compositionally unidentified.

Because Na and K are directly generated by a source process acting on the surface layer, it is natural to suspect that other species in the surface may be injected into the lunar atmosphere by this same source process. Apollo lunar sample returns have shown that several metallic species are more abundant than, or are of comparable abundance to Na and K in the lunar surface [*Taylor*, 1982]. For a surface that has reached an equilibrium under long-term bombardment by solar wind particles, one might expect that the sputtering yields of surface species reflect the bulk composition of the surface [*Johnson and Baragiola*, 1991].

If such stoichiometry holds, then a sputtered lunar atmosphere should contain metal species derived from the lunar surface in direct relation to their surface abundances. In this paper, we present results from an observational program designed to constrain the degree of stoichiometry that exists in the lunar atmosphere.

A Stoichiometric Model

Because of their significant abundances in the lunar surface and their chemical similarity to Na, we elected to first search for Ca, Ti, and Li in the lunar atmosphere. To predict resonant scattering intensities for these species based on a simple stoichiometric model, we begin with their elemental surface abundances relative to Na, which have been obtained from Apollo regolith sample returns [*Taylor*, 1982]. Assuming stoichiometric production, we computed atmospheric abundances using an exosphere model [*Chamberlain and Hunten*, 1987] at 1000 K and the photoionization loss rates of each species. We then used published oscillator strengths [*Allen*, 1973] and solar spectra

[*Kurucz et al.*, 1984] to compute the resonant scattering efficiencies g for each species. The predicted intensities are then given by

$$4\pi I = 10^{-6} g N, \quad (1)$$

where $4\pi I$ is in Rayleighs and N is the predicted line-of-sight column abundance.

The results of this calculation are shown in Table 1. The value predicted by this model for K agrees with previous observations of that species [*Potter and Morgan*, 1988a]. The intensities predicted for Ca and Ti are brighter than, or are of comparable brightness to Na and should therefore be easily detectable if the stoichiometric assumption is valid. The predicted value for Li is less easily detectable with the instrumentation we are using.

Observations

The observations analyzed in this paper are summarized in Table 2. All of the data were taken on 30 July 1994 with the McDonald Observatory 2.7 m coudé spectrograph at R≃60,000, using an 800×800-pixel CCD. Order-separating filters were used to prevent order mixing. During the observations, the Moon was 51% illuminated and ranged in zenith distance from 63° to 23°. The sky was free of clouds throughout the observing period and seeing was good (≃1″).

The observing method was as follows. Each atmospheric spectrum was taken ≃20″ above the subsolar point of the Moon's limb, with the ≃20″-long slit oriented approximately parallel to the lunar limb. For calibration purposes, spectra were also taken of the lunar surface with the slit pointed ≃20″ from the subsolar limb and oriented in the same way as the atmospheric spectra.

The 800×800-pixel CCD frames were binned 1×4, thus providing 800-pixel rows in the wavelength dimension and 200-pixel columns in the spatial dimension. The spectral range in each image was ≃8-10 Å.

Data Reduction and Analysis

Each spectrum was corrected for vignetting, bias, and pixel-to-pixel gain differences using white-lamp and dark images. Wavelength calibrations were obtained by means of a Th-Ar lamp. The Th-Ar spectra also provided a measure of the spectral resolution, which ranged from ≃50 mÅ (Ca) to 70 mÅ (Li). Spectral line tilt and curvature were corrected row-by-row through sub-pixel shifts of each row in wavelength. The spectra were then summed in the spatial dimension to provide high signal-to-noise spectra for each of the four target species. Individual atmospheric or surface spectra for each species were coadded to further increase signal-to-noise. Small, sub-pixel shifts in wavelength were required to match the positions of solar absorption features precisely.

We obtained absolute calibration of our surface spectra by computing the surface brightness of the Moon at the continuum level for the appropriate observing geometry. A constant surface albedo of 10% was assumed and a phase factor of 0.18 was computed using Hapke's lunar photometric theory [*Hapke*, 1966]. We estimate that our calibration method introduces an absolute uncertainty of ≃20%.

Calibrated spectra taken of the lunar surface and atmosphere at the Na D_1 (5896 Å) and D_2 (5890 Å) lines are shown in Fig. 1. The top panel shows a spectrum of the surface; the middle panel is a 10 minute exposure of the lunar atmosphere. Note the prominent Na emission features superimposed on the scattered lunar spectrum. The bottom panel shows the residual intensity resulting from scaling and subtracting the surface spectrum from the atmospheric spectrum. Emission line intensities of 2.8 kR (D_2) and 1.9 kR (D_1) were computed by integrating over the lines in wavelength. These intensities agree well with previous measurements of Na at ≃20″ above the subsolar point [e.g., *Potter and Morgan*, 1988a].

Residual spectra of the target species Ca I, Ti I, and Li I produced in the same manner as the Na results in Fig. 1 are shown in Fig. 2. Since no emission features are evident in these spectra, we computed upper limits on emission line intensities

as follows. First, standard deviations (σ) were computed from the residual spectra. Then we integrated artificial emission lines (gaussians) with amplitudes of 5σ and full-widths-at-half-maximum corresponding to the measured spectral resolution in the neighborhood of each line. As a result, we found 5σ upper limits of 360 R (Ca), 120 R (Ti), and 30 R (Li). These upper limits correspond to line-of-sight column abundances of 6.4×10^8 cm^{-2}, 2.1×10^8 cm^{-2}, and 2.0×10^6 cm^{-2}, respectively. When compared with the predicted column abundances in Table 1, we find that the observed upper limits fall below the stoichiometric model predictions, particularly for Ca and Ti. The implications of this result are discussed below.

Discussion

Our targeted search for resonant scattering emissions above the lunar limb has produced constraining upper limits on the abundances of Ca I, Ti I, and Li I in the lunar atmosphere. The measured upper limits on emission intensities for these species fall below the values predicted from a simple, stoichiometric model (cf., Table 1). Fig. 3 shows the degree to which the three species depart from stoichiometry. Fig. 3 also gives the ratio of the observed upper limits on atmospheric abundances to their predicted values. The upper limits for Ca and Ti are each more than an order of magnitude below predictions; the upper limit for Li is less constraining.

The non-stoichiometric results are in clear contrast to the case of atmospheric K. A comparison of the K intensity predicted from stoichiometry (Table 1) and its observed intensities [e.g., *Potter and Morgan*, 1988a] shows that K production does appear to behave stoichiometrically relative to Na.

The appearance of the volatile species Na and K in the lunar atmosphere, coupled with the absence of atmospheric counterparts of other abundant lunar surface constituents, such as Ca, Ti, and Li, is likely to be related to the details of the production mechanism(s) responsible for releasing Na and K from the surface. To be

more specific, meteoritic bombardment could sufficiently churn, or garden, the lunar surface to result in a reduced effective surface age [*Johnson and Baragiola*, 1991]. In this case solar wind sputtering yields would not approach stoichiometry and volatile species would dominate atmospheric metal abundances. Alternatively, species such as Ca and Ti may be sputtered more easily as molecular fragments (e.g., CaO, TiO, TiO_2, etc.) than as Ca or Ti atoms.

Because Ca, Ti, and Li are depleted in the lunar atmosphere relative to Na, our primary conclusion is that the release of metal vapors into the lunar atmosphere does not in general behave stoichiometrically. However, spectroscopic searches for other abundant lunar surface constituents, such as Si, Al, and Mg, should be made to obtain a more thorough understanding of the production of metallic species in the lunar atmosphere. Further observations should also be made of Ca, Ti, and Li in order to obtain detections of these species, or to produce more constraining upper limits. We plan to undertake such an observing program.

Acknowledgments. We are grateful to our colleagues Robert Johnson, Thomas Morgan, and Larry Trafton for helpful discussions. We thank William Cochran and David Doss for assistance with the observing equipment at McDonald Observatory. This research was supported by the NASA Planetary Astronomy program.

References

Allen, C. W., *Astrophysical Quantities*, Athlone, London, 1973.

Chamberlain, J. W., and D. M. Hunten, Stability of planetary atmospheres, in *Theory of Planetary Atmospheres*, pp. 330-415, Academic Press, Boston, Massachusetts, 1987.

Feldman, P. D., and D. Morrison, The Apollo 17 ultraviolet spectrometer: Lunar atmosphere measurements revisited, *Geophys. Res. Lett.*, *18*, 2105-2108, 1991.

Flynn, B. C., and M. Mendillo, Simulations of the lunar sodium atmosphere, submitted to *J. Geophys. Res.*, 1994.

Hapke, B., An improved theoretical lunar photometric function, *Astron. J.*, *71*, 333-339, 1966.

Johnson, R. E., and R. Baragiola, Lunar surface: Sputtering and secondary ion mass spectrometry, *Geophys. Res. Lett.*, *18*, 2169-2172, 1991.

Kurucz, R. L., I. Furenlid, J. Brault, and L. Testerman, *Solar Flux Atlas from 296 to 1300 nm*, Harvard University, Cambridge, 1984.

Morgan, T. H., and D. E. Shemansky, Limits to the lunar atmosphere, *J. Geophys. Res.*, *96*, 1351-1367, 1991.

Morgan, T. H., and S. A. Stern, The lunar atmosphere, *EOS*, *72*, 522, 1991.

Potter, A. E., and T. H. Morgan, Discovery of sodium and potassium vapor in the atmosphere of the Moon, *Science*, *241*, 675-680, 1988a.

Potter, A. E., and T. H. Morgan, Extended sodium exosphere of the Moon, *Geophys. Res. Lett.*, *15*, 1515-1518, 1988b.

Potter, A. E., and T. H. Morgan, Variation of lunar sodium emission intensity with phase angle, *Geophys. Res. Lett.*, *21*, 2263-2266, 1994.

Sprague, A. L., R. W. Kozlowski, D. M. Hunten, W. K. Wells, and F. A. Grosse, The sodium and potassium atmosphere of the Moon and its interaction with the surface, *Icarus*, *96*, 27-42, 1992.

Stern, S. A., and B. C. Flynn, Narrow-field imaging of the lunar sodium exosphere, *Astron. J.*, in press, 1995.

Taylor, S. R., *Planetary Science: A Lunar Perspective*, Lunar and Planetary Institute,

Houston, 1982.

This manuscript was prepared with the AGU LaTeX macros v3.1.

Figure 1. *Top*: Spectrum taken of the lunar surface 20″ from the subsolar limb. *Middle*: Spectrum taken 20″ (40 km) above the subsolar limb, showing terrestrial atmospheric scattering and superimposed lunar atmospheric emission features. *Bottom*: Difference of top and middle panels showing Na emission features at 5890 Å and 5896 Å. The signal-to-noise ratio for the D_2 line (5890 Å) is approximately 100.

Figure 2. Residual spectra, computed as in Fig. 1, for Ca, Ti, and Li. The apparent features in the Ca spectrum are artifacts due to the inelastic nature of Rayleigh scattering, resulting in a slightly blurred scattering spectrum relative to the Ca lunar surface spectrum. This effect is less apparent at longer wavelengths (e.g., Ti and Li). The upper limits on lunar atmospheric intensities are at the 5σ level. Standard deviations are 1400, 380, and 86 R $Å^{-1}$ for the Ca, Ti, and Li residual spectra, respectively.

Figure 3. *Top*: Line-of-sight column abundances at 40 km above the limb for Ca, Ti, and Li relative to Na from both the stoichiometric model (filled circles) and the observations (open circles). A typical value for K, which does behave stoichiometrically relative to Na, is also plotted. *Bottom*: Ratios of observed upper limit column abundances to predicted values. A ratio of unity indicates stoichiometric behavior relative to Na. Arrows denote that values are upper limits in the cases of Ca, Ti, and Li.

Table 1. Estimated lunar resonant scattering intensities

Species	N_{rel}[a]	N_{40}[b]	τ[c]	λ_0[d]	f[e]	πF[f]	g[g]	$4\pi I_{40}$[h]
Ca I	16	2.8×10^{10}	2.9×10^{4}	4226	1.75	96	0.56	15
Ti I	1	2.7×10^{9}	-	5035	0.18	705	0.58	1.6
Na I	1	5.4×10^{9}	5.4×10^{4}	5889	0.66	94	0.56	3.0[i]
K I	0.3	6.8×10^{8}	3.7×10^{4}	7699	0.34	238	1.6	1.1[i]
Li I	0.005	3.5×10^{6}	3.7×10^{3}	6708	0.76	1460	15	0.052

[a]Surface abundance relative to Na from Taylor (1982).

[b]Atmospheric column abundance (cm^{-2}) at 40 km above the subsolar limb at first quarter Moon based on relative surface abundance, ionization lifetime, and altitude distribution from a Chamberlain exosphere at 1000 K.

[c]Ionization lifetime (seconds).

[d]Wavelength of leading line of multiplet (Å).

[e]Oscillator strength (Allen, 1973).

[f]Solar flux at 1 AU (ergs cm^{-2} s^{-1} nm^{-1}) (Kurucz et al., 1984).

[g]Scattering efficiency ($seconds^{-1}$).

[h]Estimated emission intensity at 40 km (kR).

[i]Species has been observed via ground-based spectroscopy and/or direct imaging. Estimated intensity for this species agrees with observations (Potter and Morgan, 1988b).

Table 2. Lunar spectroscopic data from 30 July 1994

Species	UT (Start)	Exp (sec)	Target[a]
Na	08:10	600	atmosphere
	08:21	3	surface
	08:22	30	surface
Ca	08:37	30	surface
	08:41	90	surface
	08:46	1200	atmosphere
	09:12	1200	atmosphere
Ti	09:50	30	surface
	09:51	180	atmosphere
	09:54	600	atmosphere
Li	10:23	30	surface
	10:29	900	atmosphere
	10:47	1200	atmosphere

[a]Surface = 20″ from subsolar limb; Atmosphere = 20″ above subsolar limb, slit parallel to limb.

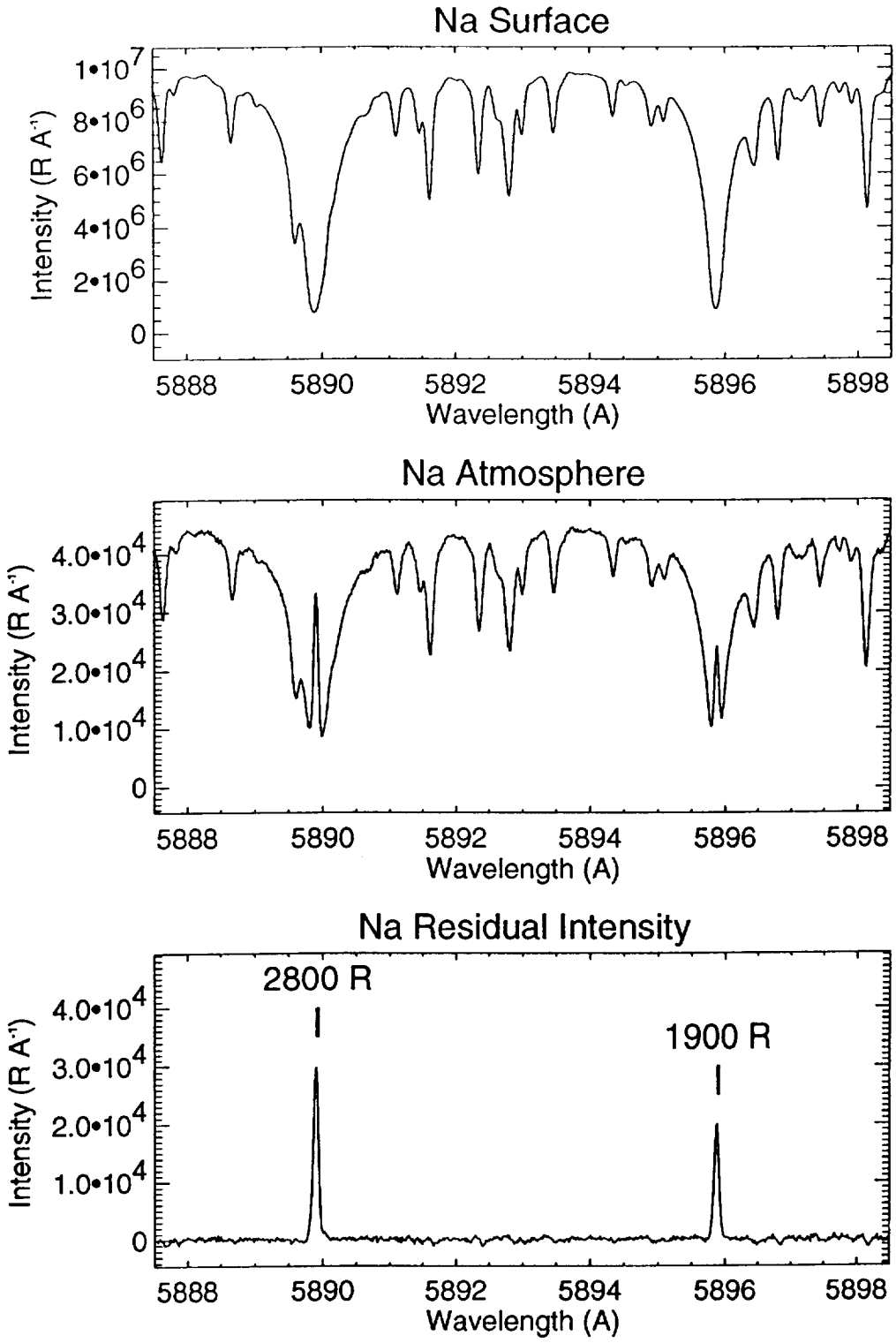
Na Surface
Intensity (R A-1)
1•10^7
8•10^6
6•10^6
4•10^6
2•10^6
0
5888
5890
5892
5894
5896
5898
Wavelength (A)
Na Atmosphere
Intensity (R A-1)
4.0•10^4
3.0•10^4
2.0•10^4
1.0•10^4
0
5888
5890
5892
5894
5896
5898
Wavelength (A)
Na Residual Intensity
2800 R
1900 R
Intensity (R A-1)
4.0•10^4
3.0•10^4
2.0•10^4
1.0•10^4
0
5888
5890
5892
5894
5896
5898
Wavelength (A)

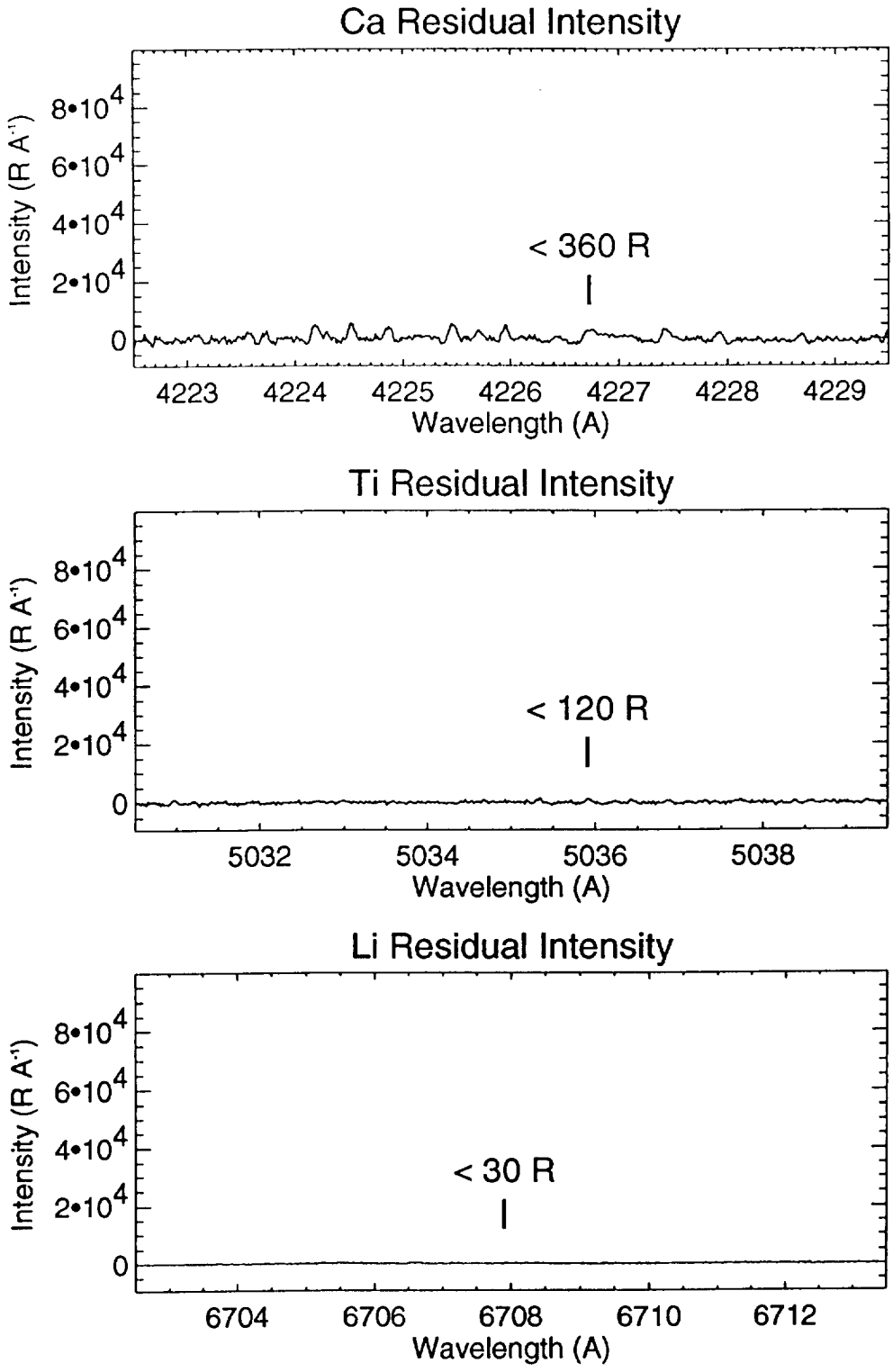
Ca Residual Intensity
Intensity (R A-1)
8•10^4
6•10^4
4•10^4
2•10^4
0
< 360 R
4223
4224
4225
4226
4227
4228
4229
Wavelength (A)
Ti Residual Intensity
Intensity (R A-1)
8•10^4
6•10^4
4•10^4
2•10^4
0
< 120 R
5032
5034
5036
5038
Wavelength (A)
Li Residual Intensity
Intensity (R A-1)
8•10^4
6•10^4
4•10^4
2•10^4
0
< 30 R
6704
6706
6708
6710
6712
Wavelength (A)

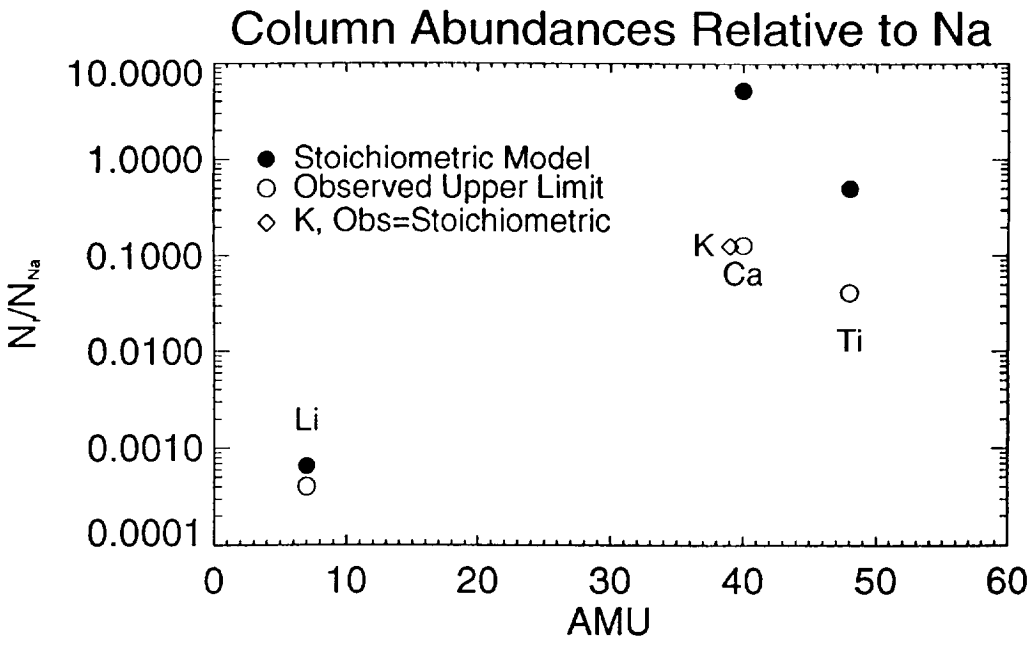
Column Abundances Relative to Na
10.0000
1.0000
0.1000
0.0100
0.0010
0.0001
N/N_Na
Stoichiometric Model
Observed Upper Limit
K, Obs=Stoichiometric
K
Ca
Ti
Li
0
10
20
30
40
50
60
AMU

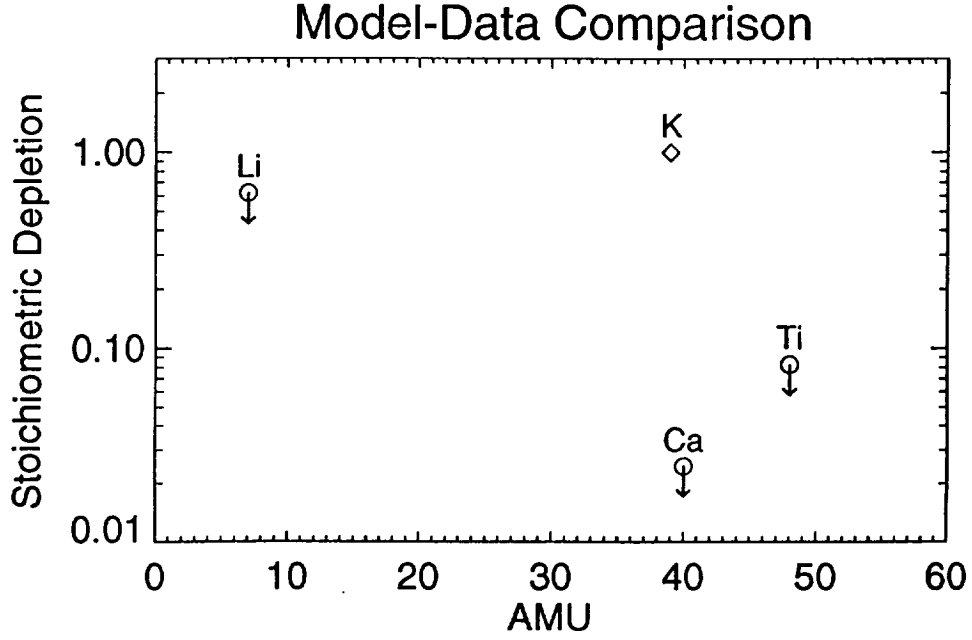
Model-Data Comparison
Stoichiometric Depletion
1.00
0.10
0.01
K
Li
Ti
Ca
0
10
20
30
40
50
60
AMU

PAPER 2

An HST Search for Magnesium in the Lunar Atmosphere

S. Alan Stern, Joel Wm. Parker, and Thomas H. Morgan
Southwest Research Institute

Brian C. Flynn
University of California at Berkeley

Donald M. Hunten and Ann Sprague
University of Arizona

Michael Mendillo
Boston University

and

Michel C. Festou
Observatoire Midi-Pyrenées

Submitted to *Icarus:* 27 November 1996
6 Manuscript pages, 1 table, 2 figures.

Running Title: Lunar Atmospheric Mg

Send Correspondence to:

Alan Stern

Southwest Research Institute

1050 Walnut St., No. 426

Boulder, CO 80302

[303]546-9670 (voice)

[303]546-9687 (fax)

alan@everest.space.swri.edu

Abstract

In October 1996 we used the Hubble Space Telescope's Faint Object Spectrograph to make the first-ever mid-ultraviolet spectroscopic search for emissions from the lunar atmosphere. This spectrum revealed no emission lines, despite the fact that strong resonance emission transitions from the Al, Si, and Mg neutrals, and Mg^+, are present in the bandpass. We derive 5 sigma upper limits on each of these species, and OH (0-0) emission. The most constraining upper limit we obtained was for Mg, which we find to be depleted relative to model predictions by a factor of 9. These findings reinforce the negative findings of our previous, ground-based search for neutral atoms in the lunar atmosphere (Flynn & Stern 1996), and suggest that Na and K may be unique in their ability to sputter from the surface as atomic neutrals. Other species may sputter away as ions or in molecular fragments.

Introduction

During the Apollo program, surface-based cold cathode gauges measured nighttime lunar atmosphere number densities as high as 10^6 cm^{-3}, but detected only He and Ar as identifiable species, with a combined peak number density near 5×10^4 cm^{-3}.

In 1988, ground-based work detected two additional lunar atmospheric species, Na and K (Potter & Morgan 1988a; Tyler et al. 1988). This landmark work renewed interest in the lunar atmosphere, in part because it enabled ground-based observations of this tenuous exosphere for the first time. The combined, near surface number density of Na and K in the lunar atmosphere is $< 10^2$ cm^{-3}. Various spectroscopic studies (e.g., Potter & Morgan 1988b; Sprague et al. 1992; Stern & Flynn 1995) have built a case that much of the lunar Na is created through energetic, nonthermal processes that populate a corona many lunar radii in diameter. These findings were most dramatically confirmed by images of the Na D lines at 5890 Å during a lunar eclipse, which directly revealed Na emission out to a distance of $\simeq$9 lunar radii (R_M; 2.3 deg) from the lunar center (Mendillo & Baumgardner 1995).

Taken together, the four known lunar atmospheric species, Ar, He, Na, and K, comprise only 5–10% of the total measured number density (cf., Morgan & Stern 1991). This fact implies that the bulk composition of the lunar atmosphere remains compositionally unknown.

A few years ago, Feldman & Morrison (1991) reanalyzed data from the Apollo 17 Ultraviolet Spectrometer (Fastie et al. 1973), and convincingly showed that C, N, O, H, CO, and Xe were not detected and cannot provide the "missing mass" of the lunar atmosphere.

More recently, Flynn & Stern (1996; hereafter F&S96) reported results from a ground-based search for potentially undiscovered lunar atmospheric metals that might be created by the same sputtering source process(es) that create Na and K. F&S96 reported constraining upper limits on a host of species, including Ti, Fe, Ca, Li, Rb, Cs, Ba, Si, and Al.

In what follows we report the results of the first survey of the 2200–3300 Å mid-UV region of the lunar atmosphere. This search yielded useful upper limits on Mg, Mg^+,

and the potentially important daughter product of H_2O, the OH radical, and new but less constraining upper limits on Al and Si.

Observations

The highly extended nature of the lunar Na corona opens the door to Hubble Space Telescope (HST) observations by allowing observations far enough from the surface to overcome the lunar avoidance angle limits of HST.

We obtained data from the HST Faint Object Spectrograph (FOS) and High Resolution Spectrograph (HRS). The FOS observations were centered at UT 1996 October 6.96 (Project GO-6513). The objective of the FOS spectrum was to obtain a low resolution (R≈100) survey spectrum of the lunar atmosphere to search for bright mid-UV emissions without bias to the possible composition of the atmosphere. The purpose of the HRS spectra, which were taken in the ∼120 minutes prior to the FOS spectrum, was to obtain more sensitive, high-resolution (R≈10,000) echelle spectra in narrow bandpasses around three particular atomic emissions: Si I (2516 Å), Mg I (2852 Å), and Al I (3092 Å). The higher spectral resolution of the HRS increases its sensitivity to faint lines over that of the FOS by reducing the "noise" contributed by scattered lunar surface continuum in the telescope.

Unfortunately, the HRS was misconfigured, causing the wrong echelle orders to be used. As a result, no useful data were obtained. Fortunately, however, the FOS dataset was properly obtained by HST, and as we describe below, it provides new and useful information.

The FOS observations were made using the FOS's BLUE digicon detector and its G270H grating, which yielded a spectrum across the 2222–3301 Å mid-UV. We observed through the largest available FOS aperture, which measures 3.66×3.7 arcsec^2, and obtained a total exposure time of 820.0 seconds.

Owing to bright object constraints, the FOS aperture was not allowed to approach closer than 0.3 deg (1.2 R_M) to the lunar limb. Figure 1 shows the path of the FOS aperture in lunar-centered coordinates during the lunar atmosphere observation of 6 October 1996.

Results

We inspected the FOS spectrum in various ways in order to search for possible emission features. The upper panel of figure 2 shows the accumulated FOS spectrum, in flux units, with a solar spectrum for comparison. As expected, the FOS spectrum consists primarily of scattered moonlight, which we verified by its lunar-like color slope. Superimposed on this scattered light signal would be any UV emission from species in the lunar atmosphere. The lower panel of this figure shows the residual created by subtracting a scaled version of the Upper Atmospheric Research Satellite/Solar Ultraviolet Irradiance Monitor (UARS/SUSIM) solar spectrum from the HST/FOS lunar spectrum. Figure 2 demonstrates that no features of interest can be detected by visual inspection of either the FOS spectrum or the residual spectrum obtained after removal of the solar spectrum by subtraction.

In Table 1 we present upper limits derived for atomic Si, Mg, Al, as well as OH, and the Mg^+ ion. These upper limits correspond to the brightness of a highly conservative, 5σ fluctuation in the local noise level at the location of each of the prospective emission features of interest.

Presented alongside the upper limits given in Table 1 are model predictions for each neutral atomic species. The predictions for the Si, Mg, and Al neutrals were derived using the stoichiometric atmosphere model and model inputs recently discussed by Flynn & Stern (1996). They correspond to the predicted brightness of each species at the time-weighted average altitude of the observations (3.1 R_M from the center, 2.1 R_M above the limb), obtained by scaling for the surface abundance, scale height, and atomic resonance fluorescence coefficient ratios relative to Na. In preparing these estimates, we assumed that these species exhibit the same ($\sim$1000 K) suprathermal density distribution that sodium does. In computing the model predictions, we corrected for the penetration of the FOS line of sight through the lunar shadow integration; this factor reduced the model brightnesses by a factor of 2 over a fully-sunlit line of sight with the same impact parameter.

The results presented in Table 1 also represent the first spectroscopic constraints

on the Mg neutral and singly-ionized Mg in the lunar atmosphere. Owing to the short lifetime of ions in the lunar atmosphere, which is open to the solar wind electric field, the nondetection of Mg^+ by the FOS is not unexpected.[1] However, the nondetection of the Mg neutral was rather unexpected, and allows us to place a strong constraint, corresponding to a 9:1 or higher depletion relative to the stoichiometric model. Although the Si and Al constraints derived from the FOS spectrum are not constraining relative to the stoichiometric model, they are consistent with the significantly more constraining ground-based results published in F&S96.

Conclusions and Interpretation

A search for resonant scattering mid-UV emissions above the lunar limb detected no spectral features. At the 5σ confidence level, these nondetections correspond to $\approx$15 R for Si I (Al 2516 Å), $\approx$19 R for the Mg II doublet (2797 Å), $\approx$53 R for Mg I (2852 Å), $\approx$74 R for Al I (3092 Å), and $\approx$67 R for OH (3085 Å). Of these, the Mg I (2852 Å) constraint provides the most significant new information.

We have found that the Mg neutral is depleted in the lunar atmosphere by a factor of at least 9, relative to stoichiometric sputtering predictions made using Na as the reference species. This of course does not eliminate the possibility of a low-energy and therefore low-altitude Mg population, but the conclusion that stoichiometric sputtering is not the source process remains valid, regardless of this possibility.

The Mg finding is in agreement with our earlier, ground-based search for a variety of other surface-derived metallic neutrals (cf., F&S96). The absence of so many stoichiometrically predicted atmospheric metal species strongly indicates that the production mechanism that is responsible for Na and K preferentially favors Na and K over other atomic neutrals.

Because of the well-established, nonthermal nature of lunar Na and K, it has been natural to suspect that a sputtering process, perhaps stoichiometric, could be responsible for generating the metal species in the lunar atmosphere. The negative results presented here and in F&S96 show that this is not the case.

---

[1] But see Hilchenbach et al. 1991 for evidence of a possible in situ detection.

This situation could occur for any of a number of reasons. One possibility is that meteoritic bombardment (Morgan & Shemansky 1991) might sufficiently gardens the lunar surface to result in a reduced effective surface age (Johnson & Baragiola 1991), and therefore a nonstoichiometric sputtering process. In this case solar wind sputtering yields would not approach stoichiometry and more volatile species like Na and K would dominate atmospheric metal abundances. A second possibility is that atmospheric recycling through photodesorption of loosely bound Na and K produces an anomalously high abundance of these two species (cf., Sprague et al. 1992; cf., also Kozlowski et al. 1990 with regard to K).

Yet another possibility concerns the nature of the chemical fragments released by the source process, whether it is sputtering, or something else. Given that (i) all of the species we have searched for here and in F&S96 are significantly depleted from stoichiometric sputtering predictions, and (ii) the fact that both solar photon and solar proton sputtering are sufficiently energetic to break chemical bonds and even to ionize some species as they are removed from the lunar surface layer, the depletions we have found may also imply that Na and K are being preferentially injected into the lunar atmosphere as atomic neutrals, while other species may be injected as atomic ions, or more likely, molecular fragments, such as MgO_x, SiO_x, and AlO_x.

We find it worthwhile to note that Na/K exospheres of Mercury and Io have also been thought to be generated in large measure by charged particle sputtering. However, like the Moon, Mercury's atmosphere has been found to be significantly depleted in both Ca (Sprague et al. 1993) and Li (Sprague et al. 1996), and Io's extended atmosphere has been found to be significantly depleted in a wide variety of metallic atomic species (Na et al. 1996). This suggests to us that the "missing" neutrals in the atmospheres of Mercury and Io may not be present themselves for the same reasons as in the case of the Moon, and heightens our interest in determining the reason for the lack of so many species once suspected to exist in all three of these atmospheres.

Acknowledgments

We thank Andy Lubenow and Melissa McGrath of the Space Telescope Science In-

stitute for their assistance in making these challenging observations. This work was supported under STScI Grant GO.6513.01-96A. The Hubble Space Telescope is operated for NASA by the Space Telescope Science Institute (STScI), a division of AURA, Inc.

References

Fatie, W.C., P.D. Feldman, R.C. Henry, H.W. Moos, and T.M. Donahue, 1973. A search for far-ultrviolet emissions from the lunar atmosphere. *Science*, **182**, 710 711.

Feldman, P., and D. Morrison, 1991. The Apollo 17 ultraviolet spectrometer: Lunar atmosphere measurements revisited, *GRL*, **18**, 2105 2108.

Flynn, B.C., and S.A. Stern, 1996. A Spectroscopic survey for metallic species in the lunar atmosphere. *Icarus*, in press.

Hilchenbach, M., D. Hovestadt, B. Klecker, and E. Mobius, 1991. Detection of singly ionized energetic lunar pick-up ions upstream of Earth's bow shock. *Proceedings of Solar Wind 7* (E. Marsch & G. Schwenn, eds.), Goslar, Germany, Pergamon Press.

Johnson, R.E., and R. Baragiola, 1991. Lunar surface: Sputtering and secondary ion mass spectrometry, *GRL*, **18**, 2169-2172.

Kozlowski, R.W.H., Tyler, A.L., and D.M. Hunten, 1990. An extended potassium componsent in the lunar exosphere. *GRL*, **19**, 642–646.

Mendillo, M., and J. Baumgardner, 1995. Detection of the moon's extended atmosphere during solar eclipse. *Nature*, **377**, 404–406.

Morgan, T.H., and D.E. Shemansky, 1991. Limits to the lunar atmosphere, *JGR*, **96**, 1351–1367.

Morgan, T.H., and S.A. Stern, 1991. Revived interest in the lunar atmosphere, *EOS*, **72**, 225-228..

Na, C.Y., E.S. Barker, L.M. Trafton, and S.A. Stern, 1996. A search for new species abundances in Io's extended atmosphere. *Icarus*, submitted.

Potter, A.E., and T.H. Morgan, 1988a. Discovery of sodium and potassium vapour in the atmosphere of the Moon. *Science*, **241**, 675–680.

Potter, A.E., and T.H. Morgan, 1988b. Extended sodium exosphere of the Moon. *GRL*, **15**, 1515 1518.

Sprague, A.L., R.W. Kozlowski, D.M. Hunten, W.K. Wells, and F.A. Grosse, 1992. The sodium and potassium atmosphere of the Moon and its interaction with the surface, *Icarus*, **96**, 27 42.

Sprague, A.L., R.W. Kozlowski, D.M. Hunten, and F.A. Grosse, 1993. An Upper Limit on neutral calcium in Mercury's atmosphere. *Icarus*, **104**, 33–37.

Sprague, A.L., D.M. Hunten, and F.A. Grosse, 1996. Upper limit for lithium in Mercury's atmosphere. *Icarus*, **124**, 345–349.

Stern, S.A., and B.C. Flynn, 1995. Narrow-field imaging of the lunar sodium exosphere. *AJ*, **109**, 835–841.

Tyler, A.L., R.W. Kozlowski, and D.M. Hunten, 1988. Observations of sodium in the tenuous lunar atmosphere. *GRL*, **15**, 1141–1144.

Table 1

Comparison of FOS Upper Limits to Model Predictions

Species	λ_0	Upper Limit Brightness	Model Brightness ($3.1\ R_M$)
Si I	2516 Å	15 R	002 R
Mg II	2797 Å	19 R	N/A
Mg I	2852 Å	53 R	476 R
Al I	3092 Å	74 R	002 R
OH (0-0)	3085 Å	67 R	N/A

The observed upper limits are for a spectral binning equal to the 25 Å resolution of the filled FOS slit with the G270H grating. Model-predicted brightnesses (cf., F&S96 for model details) were computed for an impact parameter of 3.1 R_M from the lunar center, for the shadow geometry of our observations. The stoichiometric model does not meaningfully predict the brightness of either OH or the Mg^+ ion.

Figure Captions

Figure 1. The geometry of the 1996 October 6.9 lunar atmosphere HST observations. North is up. The illuminated portion of the Moon is to the right (west) of the terminator. The trajectory of the FOS aperture around the Moon was created primarily by the changing parallax of the Moon as seen from HST during the observation.

Figure 2. Upper panel: The flux spectrum obtained by the FOS near the Moon on 1996 October 6.9 (solid line, with error bars), compared to the average of three full-disk solar spectra obtained by the UARS SUSIM instrument on 1996 Oct 5–7, binned to the FOS resolution (dotted line). The solar spectrum has been shifted by a constant multiplier to fit on the same scale as the lunar spectrum. The FOS spectrum consists of scattered moonlight, and reveals no obvious atmospheric emissions. *Lower panel:* the residual spectrum created by subtracting an appropriated scaled version of the UARS SUSIM solar spectrum shown in the upper panel, from the HST/FOS lunar atmosphere spectrum. Error bars were derived from the HST spectrum alone, since we have not information on the UARS spectrum error budget; true quadrature sums of FOS+UARS errors would be larger. The lack of species detection is clear.

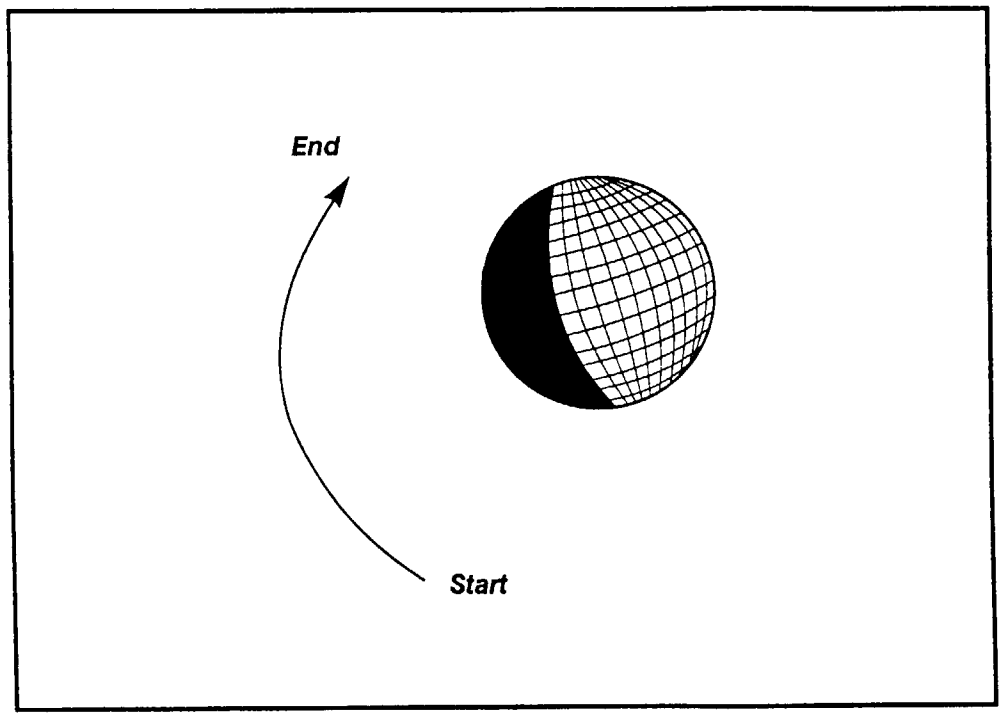
End
Start

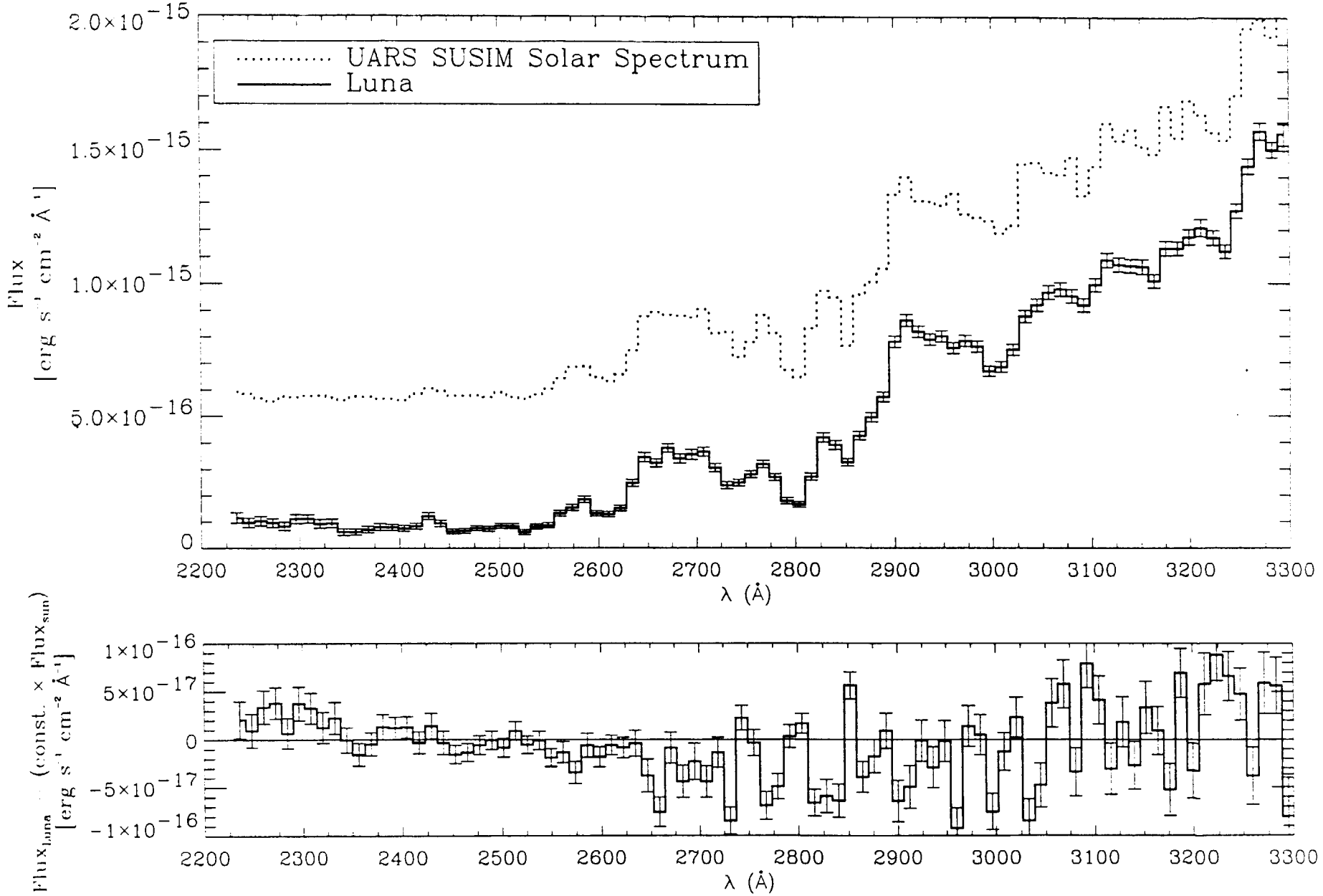
UARS SUSIM Solar Spectrum
Luna
Flux
[erg s⁻¹ cm⁻² Å⁻¹]
2.0×10⁻¹⁵
1.5×10⁻¹⁵
1.0×10⁻¹⁵
5.0×10⁻¹⁶
0
2200
2300
2400
2500
2600
2700
2800
2900
3000
3100
3200
3300
λ (Å)
Flux_Luna − (const. × Flux_sun)
[erg s⁻¹ cm⁻² Å⁻¹]
1×10⁻¹⁶
5×10⁻¹⁷
0
-5×10⁻¹⁷
-1×10⁻¹⁶
2200
2300
2400
2500
2600
2700
2800
2900
3000
3100
3200
3300
λ (Å)